CONF-9106146--1

An invited paper submitted to Sixth JIM International Symposium (JIMIS-6) on Intermetallic Compounds — Structure and Mechanical Properties, June 17-20, 1991, Sendai, Japan

EFFECTS OF ELASTIC ANISOTROPY ON MECHANICAL BEHAVIOR OF INTERMETALLIC COMPOUNDS*

CONF-9106146--1

DE91 010392

M. H. Yoo

Metals and Ceramics Division, Oak Ridge National Laboratory
Oak Ridge, TN 37831-6115 U.S.A.

Fundamental aspects of the deformation and fracture behavior of ordered intermetallic compounds are examined within the framework of linear anisotropic elasticity theory of dislocations and cracks. The orientation dependence and the tension/compression asymmetry of yield stress are explained in terms of the anisotropic coupling effect of non-glide stresses to the glide strain. The anomalous yield behavior is related to the disparity (edge/screw) of dislocation mobility and the critical stress required for the dislocation multiplication mechanism of Frank-Read type. The slip-twin conjugate relationship, extensive faulting, and pseudo-twinning (martensitic transformation) at a crack tip can be enhanced also by the anisotropic coupling effect, which may lead to transformation toughening of shear type.

1. Introduction

For several decades now there have been many research activities aimed at understanding the peculiar mechanical behavior exhibited by ordered intermetallic compounds, e.g., pseudo-elasticity, anomalous yielding and work-hardening, shape memory effects, and extreme brittleness of grain boundaries. Isotropic elasticity is generally used to describe the stability of dislocations and cracks although very few intermetallic compounds actually come near this approximation. It is the purpose of this overview paper to assess the physical sources for the peculiar mechanical behavior within the framework of anisotropic elasticity theory.

It is now generally accepted that the mobility of superdislocations in the $L1_2$- and B2-type structures is usually controlled by the dislocation core structure [1]. The commonly observed Schmid's law violation and the tension/compression asymmetry of critical resolved shear stress (CRSS) can be interpreted on the basis of the non-planar core structures predicted by atomistic simulation studies in the $L1_2$-type [2-4] and the B2-type structures [5,6]. Obviously, such an atomistic detail of dislocation core structures is beyond the scope of the elasticity theory of dislocations. Nevertheless, the shortcomings of the continuum mechanics approach can be overcome, to a certain extent, when principles such as Newton's third law, crystal symmetry, and superposition of infinitesimal virtual dislocations are brought into the problem.

Using anisotropic elasticity, Duesbery [7] introduced the concept of "force doublets" in order to account for the non-planar core structures of dislocations in the fcc and bcc structures. Extending this concept to the dissociation reactions of superdislocations in the $L1_2$-and B2-type structures, Yoo et al. [8] developed the force couplet model (FCM) to predict the yield strength anomaly reported in Ni_3Al and CuZn. The orientation dependences of CRSS reported in B2 alloys (FeAl, AgMg, and CuZn) at low temperatures were qualitatively predicted using the modified Peierls-Nabarro model on the basis of the anisotropic coupling effect of non-glide stresses [9,10].

It is attempted, in this overview, to bring together fundamental concepts required for understanding the deformation and fracture behavior unique to the ordered superlattice structures without a detailed exposition of the theory and experimental results. First, available elastic

* Research sponsored by the Division of Materials Science, U.S. Department of Energy under contract DE-AC05-84OR21400 with Martin Marietta Energy Systems, Inc.

constants are collected in Sec. 2. Effects of the elastic anisotropy on the dissociation reactions of <110> and <111> superdislocations are discussed in Secs. 3 and 4, respectively. Section 5 on yield strength includes the role of dislocation sources and multiplication mechanisms. The role of extensive faulting or microtwinning in crack tip plasticity is treated in Sec. 6. Finally, Sec. 7 includes a brief discussion of the intrinsic brittleness of grain boundaries.

2. Elastic Constants

In a crystal of cubic symmetry, there exist three independent elastic constants — c_{11}, c_{12}, and c_{44} stiffness constants or s_{11}, s_{12}, and s_{44} compliance constants [11]. The range of elastic anisotropy can be exhibited in a $1/\sqrt{A}$ vs. ν plot [12], where $\nu = -s_{12}/s_{11} = c_{12}/(c_{11} + c_{12})$ is Poisson's ratio and $A = 2(s_{11}-s_{12})/s_{44} = 2c_{44}/(c_{11}-c_{12})$ is Zener's ratio. Twenty-two ordered intermetallic compounds, belonging to the four structure types ($L1_2$, B2, DO_3 and $L2_1$), are shown in such a plot (Fig. 1). Those underlined are from the calculated data at 0 K [10,13,14], and the rest are from the available experimental data at room temperature [15-17].

The postulate that the elastic strain energy must be positive, for otherwise the crystal would be unstable, gives the following restrictions on the three constants [11]: $c_{44} > 0$, $c_{11} > |c_{12}|$, and $c_{11} + 2c_{12} > 0$. These stability requirements impose limitations on the allowed range of values of A and ν (i.e., $0 < A < \infty$ and $-1 < \nu < 1/2$). All, but Al_3Sc, show $A > 1$. For metals ν lies usually between 0.25 and 0.45. Again, Al_3Sc is an exception with $\nu = 0.19$. The implication of such a low value of ν in dislocation multiplication processes will be discussed in Sec. 5.

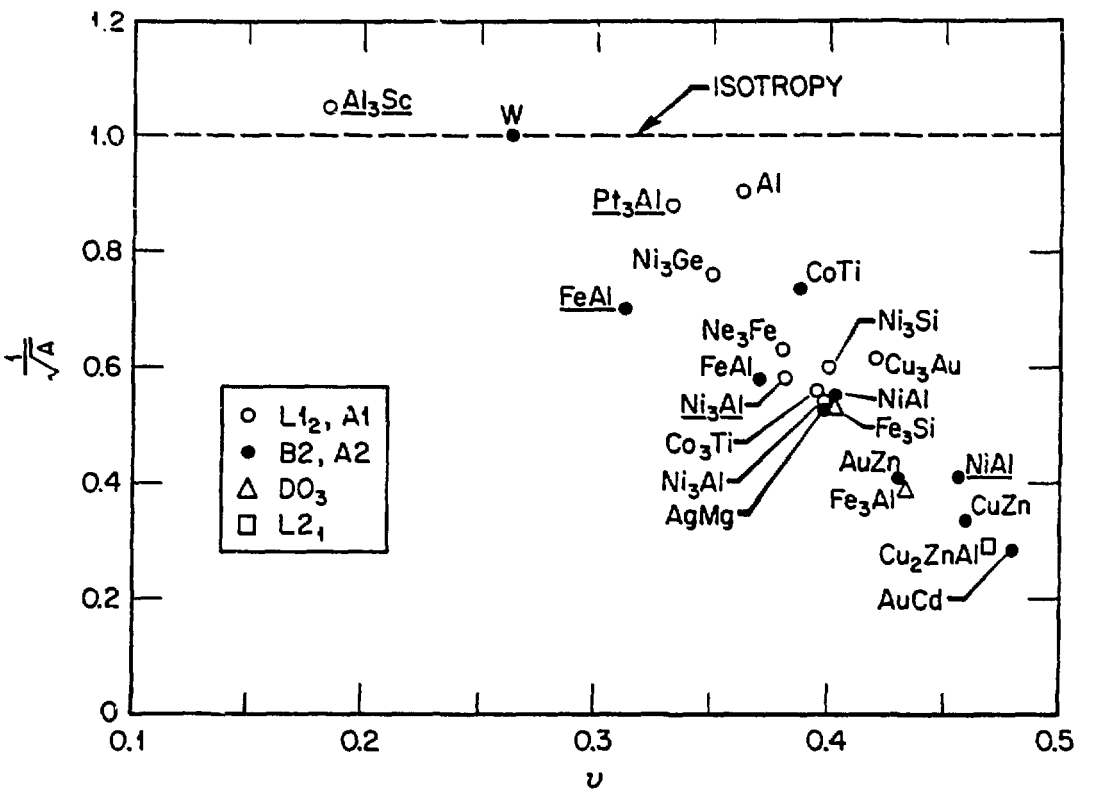

Fig. 1. Elastic properties of 20 intermetallic compounds of the cubic structures in a $1/\sqrt{A}$ vs. ν plot. Those underlined are from the calculated data at 0 K.

Composition and temperature dependences of the elastic constants are available for NiAl [18,19], FeAl [20], and CuZn [21]. As these alloys become rich in the transition (or noble) metal element, both A and ν increase toward the lower right-hand corner of Fig. 1. In the nickel-rich NiAl alloys, the decrease in $c' = (c_{11} - c_{12})/2$ with increasing nickel content and/or decreasing temperature is indicative of lattice instability [18]. This leads to an ease of shearing on the {110} planes stacking along the <110> directions, and the various stacking sequences of the {110} planes result in different martensitic structures [22]. For the relationships between elastic constants and lattice instabilities the readers are referred to an excellent review by Nakanishi [23].

3. <110> Dislocations

Consider the plane problem for a crystal which possesses at least one two-fold symmetry axis (e.g, a <110> axis in cubic crystals) and let the x_3-axis of the Cartesian coordinate system be parallel to it. Then the generalized Hooke's law for stress-strain (σ - ε) relationships may be given as

$$\begin{bmatrix} \varepsilon_1 \\ \varepsilon_2 \\ \varepsilon_6 \\ \hline \varepsilon_4 \\ \varepsilon_5 \end{bmatrix} = \left[\begin{array}{ccc:cc} S_{11} & S_{12} & S_{16} & 0 & 0 \\ S_{12} & S_{22} & S_{26} & 0 & 0 \\ S_{16} & S_{26} & S_{66} & 0 & 0 \\ \hline 0 & 0 & 0 & S_{44} & S_{45} \\ 0 & 0 & 0 & S_{45} & S_{55} \end{array}\right] \begin{bmatrix} \sigma_1 \\ \sigma_2 \\ \sigma_6 \\ \hline \sigma_4 \\ \sigma_5 \end{bmatrix}, \qquad (1)$$

where S_{ij} is the modified elastic compliance [24]. The modified compliance matrix is partitioned into the plane strain (upper-left) and the anti-plane strain (lower-right) parts. Now, if a dislocation line (or a crack line) lies parallel to the x_3 axis, the former is for an edge dislocation (or Mode I or II crack) and the latter is for a screw dislocation (or Mode III crack).

Table 1 lists the four examples of an edge dislocation. The anisotropic coupling effect of normal stress (σ_1 for the $L1_2$ structure or σ_2 for the B2 structure) on the glide strain, ε_6, is $S_{16}/S_{66} = 0.15$ for Ni_3Al or $S_{26}/S_{66} = 0.19$ for CuZn. According to the calculated elastic constants of TiAl [25] and $TiAl_3$ [14], the magnitudes of S_{16} and S_{26} are comparable and their signs are opposite (Table 1). This means that the principal axes of the pure shear strain are rotated (about the x_3-axis) with respect to those of the shear stresses by a large angle (>10°). The effect of the resolved normal stress on the twin plane was found to increase the glide strain for microtwinning at a Mode-I crack tip of (110) type in TiAl [26].

Table 1. The modified compliance constants for an edge dislocation of $\{111\}\langle 11\bar{2}\rangle$ and $\{11\bar{2}\}\langle 111\rangle$ types

Alloy	Slip or Twin System	10^{-11} m^2/N		
		S_{66}	S_{16}	S_{26}
Ni_3Al	$\{111\}\langle 11\bar{2}\rangle$	1.65	0.24	0.06
CuZn	$\{11\bar{2}\}\langle 111\rangle$	3.62	-0.18	0.67
TiAl	$(111)[11\bar{2}]$	2.00	-0.24	0.19
$TiAl_3$	$(111)[11\bar{2}]$	1.71	0.75	-0.81

When a superdislocation of pure edge or screw character splits into two superpartials with identical Burgers vectors, the angular component of the interaction force, F_θ, generally exists because of the anisotropic coupling effect (i.e., $S_{16} \neq 0$, $S_{26} \neq 0$ for edge and $S_{45} \neq 0$ for screw). Schematic diagrams are shown in Fig. 2. The relative strength of the interaction torque, F_θ/F_r, can be obtained numerically, or analytically in the case of screw dislocations, in terms of the elastic constants [27]. Some numerical values of F_θ/F_r are, for example, 0.12 for $(11\bar{2}2)\langle\bar{1}\bar{1}26\rangle$ edge in Ti_3Al [28], 0.26 for $(11\bar{2})\langle 111\rangle$ edge in CuZn [8], and 0.62 for $(111)\langle\bar{1}01\rangle$ screw in Ni_3Al [8]. If the x_1 or x_2 axis is also parallel to a two fold symmetry axis of the crystal, then F_θ vanishes.

For a static equilibrium of the dissociated superdislocations, the so-called couple stress [29] due to F_θ is counter balanced by the force couplets which may be modelled by the fractional edge dislocation pair of opposite sign as shown in Fig. 2. The glide stress component, σ_6 (or σ_4), of an applied stress exerts a driving force on each edge (or each screw) dislocation according to the Peach-Koehler formula [30]. In addition, the signs and magnitudes of the non-glide stress components as shown in Figs. 2 (a and b) cause expansion (or contraction) of the force couplets, thus contributing to the orientation dependence and the tension/compression asymmetry of the CRSS.

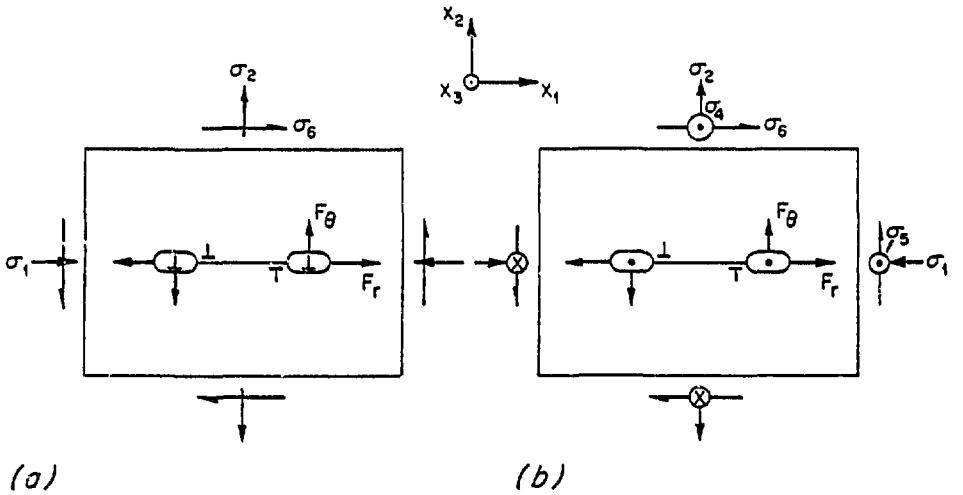

Fig. 2. Definition of the force couplets and the fractional edge dislocation pairs for the dissociated superdislocations of (a) edge and (b) screw type along the $[\bar{1}01]$ axis.

4. <111> Dislocations

Consider the anti-plane strain problem of a [111] screw dislocation in the B2 structure. The pertinent stress-strain relationships with respect to $(1\bar{1}0)$ and $(11\bar{2})$ planes are

$$\varepsilon_4 = S_{44}\sigma_4 + S_{46}\sigma_6 , \tag{2}$$

$$\varepsilon_5 = S_{15}\sigma_1 + S_{25}\sigma_2 + S_{55}\sigma_5 , \tag{3}$$

where $S_{44} = S_{55} = s_{44} + 4\delta/3$, $S_{46} = -2S_{15} = 2S_{25} = 2\delta\sqrt{2}/3$, and $\delta = s_{11} - s_{12} - s_{44}/2$. The anisotropy factor diminishes to zero upon approaching the elastic isotropy, i.e., $\delta \rightarrow 0$, $A \rightarrow 1$. The δ values of 0.32 and 4.54 for FeAl [10] and CuZn-I [8] give $S_{46}/S_{44} = 0.29$ and 0.59 and $S_{15}/S_{55} = -0.15$ and -0.29, respectively. No interaction torque exists between a pair of 1/2[111] superpartials when they are lying on $(1\bar{1}0)$ or $(11\bar{2})$ planes [31]. Therefore, the core transformation of individual superpartials may be the most important factor controlling the dislocation mobility, as in the case of bcc metals, followed by the fault (APB) dragging effect [8].

The distribution of displacement component perpendicular to the [111] dislocation, which arises due to the elastic anisotropy [32], is shown in Fig. 3(a). This displacement field may be regarded as a corrugation of the cylindrical surface (the dashed circle) by a distribution of infinitesimal edge dislocations [8] as shown in Fig. 3(b). The glide stress component σ_4 (or σ_5) of an applied stress exerts a driving force on the screw dislocation along the $(\bar{1}01)$ plane [or the $(\bar{1}2\bar{1})$ plane]. The non-glide stress components, the so-called edge stresses [7], distort the three-fold symmetry into one which is relatively more planar with respect to a potential slip plane. A numerical factor of the anisotropic coupling effect of non-glide stress components is given as $\alpha = \Sigma (S_{i4}/S_{44})(\sigma_i/\sigma_4)$ summing over all the non-glide stress components i = 1,2,--,6 except i = 4 for the glide stress, σ_4. Using the elastic constants of FeAl calculated at 0 K [10], we obtain the orientation dependence of α under a compressive applied stress as shown in Fig. 4(a).

The operative slip systems in Fe-Al (48 at. %) single crystals at 77 K were reported by Yamagata and Yoshida [33]. Figure 4(b) shows the three reported values of CRSS, τ_c. An estimate of CRSS for 1/2[111] screw dislocations can be made using the Peierls-Nabarro model, $\tau_p = 2K_s \exp(-2\pi \zeta/b)$, where ζ is a measure of the dislocation core (planar) width [34], and K_s is the energy factor. The "ease-of-gliding" parameter, ζ/b, is modified by $(1 + \alpha)\zeta/b$ due to the anisotropic coupling effect (i.e., the larger the increase in glide strain due to the non-glide stresses, the higher the value of ease-of-gliding parameter, and hence, the lower the modified Peierls stress, τ_c). Calculated results for τ_c are shown in Fig. 4(b). Comparing with the experimental data, the calculated orientation dependence of τ_c shows good qualitative agreement (i.e., slip occurs on the $(\bar{2}11)$ twinning plane). Reversing the sense of the applied stress inverts the symmetry of τ_c-χ curve, and hence, predicts the correct tension/compression asymmetry of CRSS.

5. Yield Strength

The anomalous (positive) temperature dependence of yield strength with increasing temperatures is well documented for intermetallic compounds, especially of the $L1_2$ structure [35]. In the $(111)[10\bar{1}]$ slip of Ni_3Al, this anomaly is usually found when the yield stress is measured at a macrostrain, $\varepsilon > 10^{-4}$, but not at a microstrain range $\varepsilon = 10^{-6}$ - 10^{-5} [36,37]. An explanation of this observation was offered by Kear and Oblak [38] on the basis of the disparity of dislocation mobility between the edge and screw segments. Effects of the elastic anisotropy on the disparity can be assessed in terms of the ratio of ζ/b [34], i.e., $K_e S_{66}/K_s S_{44}$, and of F_θ/F_r, i.e., $F_\theta/F_r = \sqrt{2}(A - 1)/(A + 2)$ for the screw and $F_\theta = 0$ for the edge orientation [39]. Table 2 lists these ratios for five $L1_2$ alloys. The two extreme cases are noteworthy, i.e., Ni_3Al and Al_3Sc.

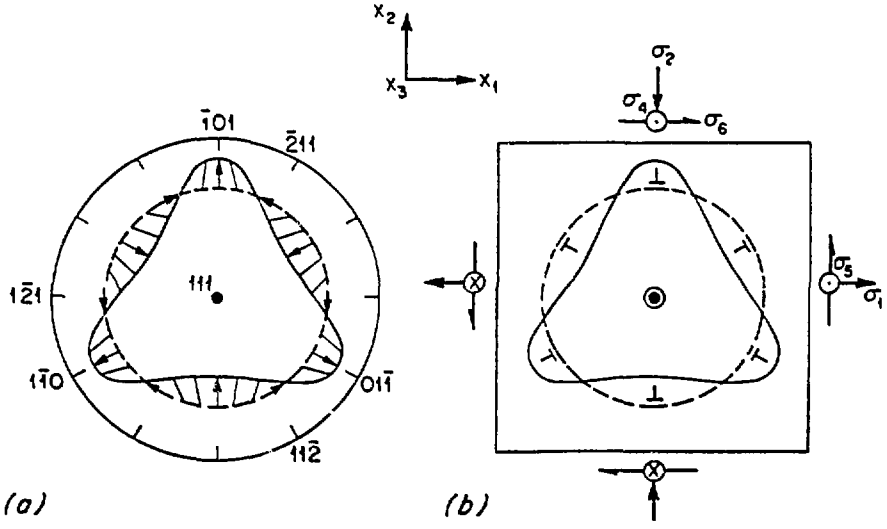

Fig. 3. [111] screw dislocation core structure (a) displacement normal to the dislocation line and (b) glide and non-glide stress components.

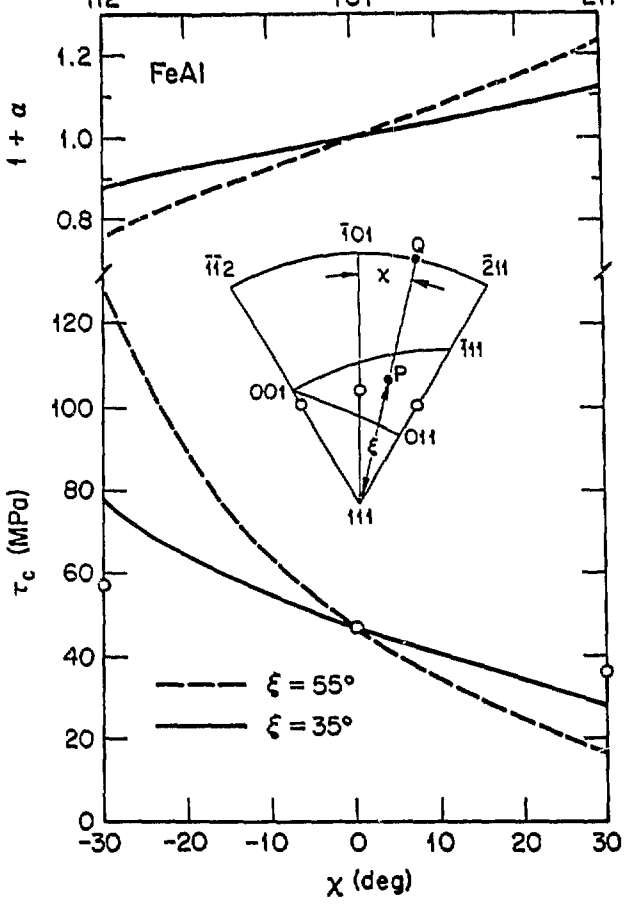

Fig. 4. Orientation dependences of (a) anisotropic coupling effect $1 + \alpha$ and (b) modified Peierls stress τ_c for FeAl at 0 K. Three open symbols are the experimental data of Fe-48% Al at 77 K [33].

Table 2. Elastic anisotropy effects on disparity (edge/screw) of superdislocation mobility of (111)[$\bar{1}$01] slip in the $L1_2$ structure

Alloy	A	$\frac{1}{1-\nu}$	$\frac{K_e S_{66}}{K_s S_{44}}$	$\frac{F_\theta}{F_r}$
Ni_3Al	3.33	1.66	1.66	0.62
Cu_3Au	2.62	1.72	1.76	0.50
Ni_3Fe	2.53	1.60	1.57	0.48
Pt_3Al	1.30	1.50	1.49	0.13
Al_3Sc	0.90	1.22	1.24	0.05

In Ni_3Al, since the disparity indicated by $K_e S_{66}/K_s S_{44} = 1.66$ is further increased by the presence of interaction torque, the FCM reinforces the basis for the explanation that the micro-yielding observed is presumably because of the glide interaction between the edge segments of a grown-in dislocation density. When the total strain increases ($\varepsilon \gtrsim 10^{-4}$), however, as in the case of the yield stress determination by 0.2% offset method, it is necessary to invoke suitable sources and multiplication mechanisms for an appropriate mobile dislocation density. Elastic anisotropy effects on a dislocation-multiplication of Frank-Read type may be discussed with the aid of Fig. 5. The

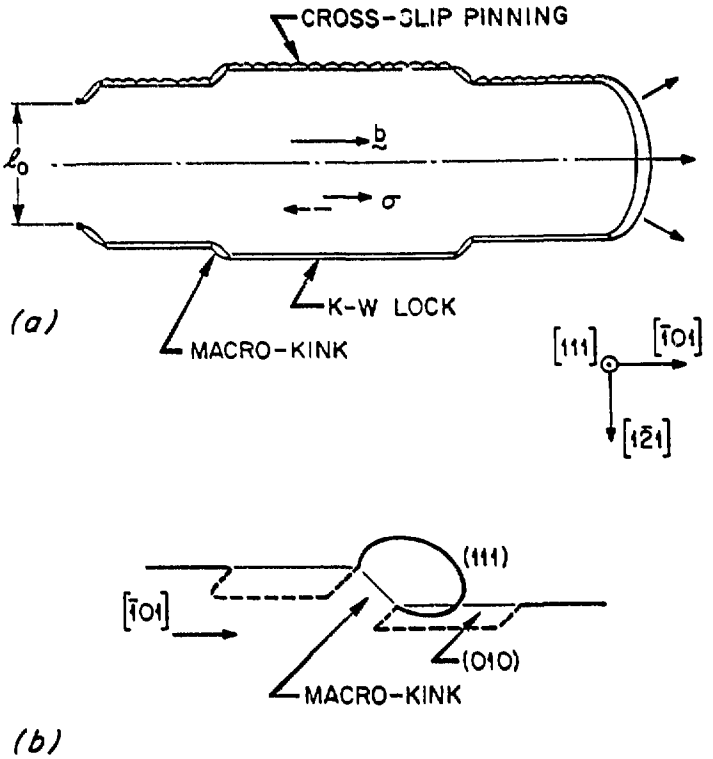

Fig. 5. Frank-Read loop formation from (a) a primary source with the anchor points of separation ℓ_0 and (b) the secondary source of a macro-kink.

equilibrium shape of a (111)[$\bar{1}$01] glide loop is an ellipse with the ratio of major/minor axis of K_e/K_s, or $1/(1 - \nu)$. A potential Frank-Read (F-R) source with the unspecified anchoring points of ℓ_0 interspacing is shown in Fig. 5(a). Under an applied stress, this F-R loop will extend preferentially along the [$\bar{1}$01] direction because of the cross-slip pinning (CSP) events [the top-half of Fig. 5(a)] [40] or the Kear-Wilsdorf (K-W) locks [the bottom-half of Fig. 5(b)] [41]. Consequently, a macro-yield strength measured at $\varepsilon > 10^{-4}$ must be controlled by the stress required to expand the primary F-R loop beyond a critical minor radius. A secondary F-R loop formation from a macro-kink [Fig. 5(b)] is possible, but the critical stress in this case would be higher than for Fig. 5(a).

In Al_3Sc, on the other hand, no yield anomaly is expected to occur insofar as the elastic anisotropy effect is concerned, viz., the major driving force for the CSP mechanism [42] is nearly zero, $F_\theta/F_r = 0.05$. Moreover, the relatively low yield strength of Al_3Sc [43] may be explained in terms of the nearly circular F-R loop expected from the unusually low value of $\nu = 0.19$.

6. Cleavage Fracture

Under the plane problem described in Sec. 3, the anisotropic solutions for the stress field at a crack tip were obtained by Sih et al. [44]. The calculated stress fields at a Mode-I crack tip of (110) type in TiAl are shown in Fig. 6. The effect of elastic anisotropy on the normal σ_θ and shear $\tau_{r\theta}$ stress fields are shown in Figs. 6 (a and b), respectively. Figure 7 shows the elastic strain field $\varepsilon_{r\theta}$ with (closed symbols) and without (open symbols) the anisotropic coupling effect of σ_θ. Also included in Fig. 7 are the specific values of $\varepsilon_{r\theta}$ for the (111)[11$\bar{2}$] primary twins (T), the (111)[$\bar{1}\bar{1}$2] complementary twins (T′), and the conjugate (001)1/2[1$\bar{1}$0] slip (S). This slip-twin conjugate relationship [45,46] as well as the primary ordered twinning contribute to the strain compatibility for localized plasticity at a crack tip of Mode-I type [26].

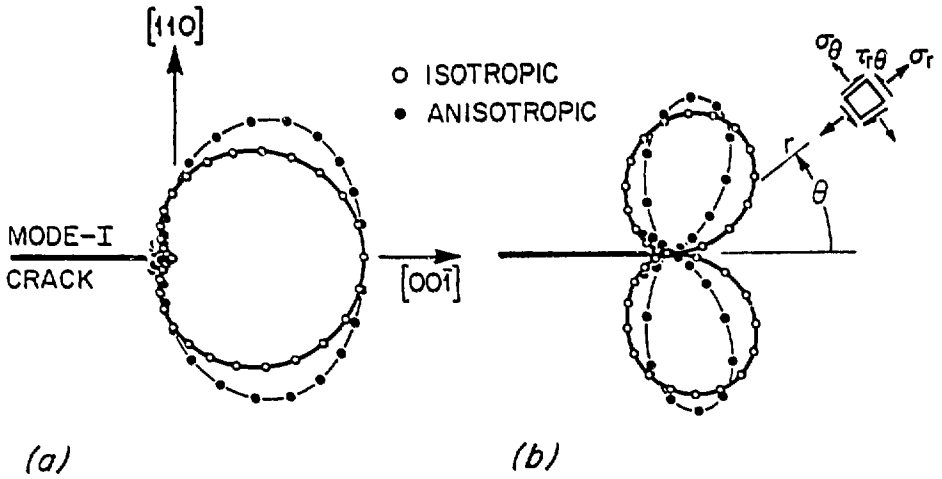

Fig. 6. Stress field at a Mode-I crack tip of (110) type in TiAl. (a) Normal stress σ_θ and (b) shear stress $\tau_{r\theta}$.

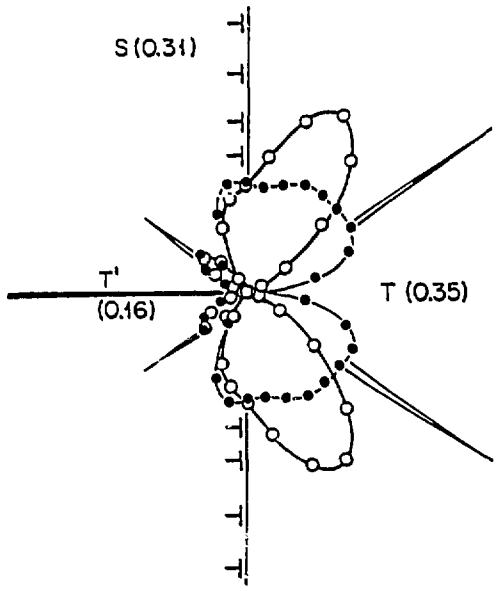

Fig. 7. Elastic shear strain field at a Mode-I crack tip of (110) type in TiAl, including the anisotropic coupling effect of σ_θ.

7. Discussion

In any crystalline lattice, the force opposing dislocation motion is an intrinsic physical property of the dislocation lattice, which must have symmetry at least equal to that of the point group of the dislocated crystal [Neumann's principal [11]]. In an ordered superlattice, it is therefore important to discuss the symmetry relationship between the interaction torque and the antiphase boundary (APB) energy. The stability of (111) APB in the $L1_2$ structure and (11$\bar{2}$) APB in the B2 structure was investigated earlier by Yamaguchi et al. [47,48], using γ-surface calculations. The conclusions were that the (111) APB can be stable with a fault vector, 1/2[$\bar{1}$01] $\pm \chi/6[1\bar{2}1]$, and the (11$\bar{2}$)APB with 1/2[111] $\pm \chi'/6[111]$, where χ and χ', are in the range of 1/5 to 1/6. These are entirely consistent with the premise of the FCM, viz. the fractional edge dislocation pairs on the APB interface shown in Figs. 2 (a and b).

The actual magnitudes of shear fault energies (e.g. APB, SISF) of a specific ordered intermetallic alloy dictate the applicability of the FCM. In the two extreme cases of a low APB energy (e.g., Cu_3Au at temperatures near its T_c = 661 K) or a high APB energy (e.g., 670 mJm^2 for Al_3Sc [14]), the superpartial or the total superdislocation should be treated independently and as such the effect of elastic anisotropy, or the lack of it, must be analyzed. It is the intermediate regime of APB energy (e.g., ~100 mJ/m^2 for Ni_3Al and ~50 mJ/m^2 for CuZn), for which the FCM for yield and flow mechanisms has been developed [8,39,42].

The role of the anisotropic coupling effect in crack tip plasticity can be analyzed in a wider range of ordered alloys. The reported cleavage habit planes of {110} for NiAl and {100} for FeAl are interpreted in terms of their cleavage energies and elastic anisotropy. In $L1_2$ alloys with a low SISF energy (e.g., Ni_3Al and Co_3Ti), extended stacking faults make a significant contribution to the energy dissipation process at a crack tip. In all cases, the effect of the resolved normal stress on the habit plane of superpartials is to enhance extensive faulting or microtwinning at a crack tip, leading to transformation toughening of shear type. These results along with the intrinsic brittle-to-ductile transition phenomena reported in TiAl and NiAl and the extrinsic effect of boron additions on room temperature ductility of Ni_3Al will be presented elsewhere.

Finally, as for the role of elastic anisotropy in intergranular brittle fracture, the competitive process between intergranular cracking and slip initiation from the grain boundary under a stress concentration deserves much further investigation [49]. Recently, finite element modeling based on anisotropic elasticity was successfully used to predict the experimentally observed initiation of (111) slip from aluminum bicrystals and multicrystals [50]. Since all of the intermetallic alloys show much greater elastic anisotropy than aluminum (Fig. 1), the effect of elastic incompatibility on the stress concentration at a grain-boundary junction is expected to be relatively more pronounced in ordered intermetallic alloys.

Acknowledgments

The author would like to thank C. L. Fu and E. P. George for helpful discussions, T. Takasugi for releasing the elastic constant data on $Ni_3(Si,Ti)$, $Ni_3(Al,Ti)$, and Ni_3Ge before publication, and C. L. Dowker for manuscript preparation.

References

[1] V. Vitek: Dislocation and Properties of Real Materials, The Inst. of Metals, London, (1985) 30.
[2] M. Yamaguchi, V. Paidar, V. Vitek, and D. P. Pope: Phil. Mag. A, 45 (1982) 867.
[3] D. Farkas and E. J. Savino: Scripta Met., 22 (1988) 557.
[4] M. H. Yoo, M. S. Daw, and M. I. Baskes: Atomistic Simulation of Materials: Beyond Pair Potentials, Ed. by V. Vitek and D. J. Srolovitz, Plenum Press, New York, (1989) 401.
[5] S. Takeuchi: Phil. Mag. A, 41 (1980) 541.
[6] M. Yamaguchi and Y. Umakoshi: Structure and Properties of Crystal Defects, Ed. by V. Paidar and L. Lejcek, Elsevier, Amsterdam, (1984) 131.
[7] M. S. Duesbery: Acta. Met., 31 (1983) 429.
[8] M. H. Yoo, J. A. Horton, and C. T. Liu: Acta Met., 36 (1988) 2935.
[9] M. H. Yoo, T. Takasugi, S. Hanada, and O. Izumi: Mater. Trans. JIM, 31 (1990) 435.
[10] C. L. Fu and M. H. Yoo: Acta. Met. (submitted).
[11] J. F. Nye: Physical Properties of Crystals, Clarendon Press, Oxford, (1957) 137, 20.
[12] J. W. Steeds: Arisotropic Elasticity Theory of Dislocations, Clarendon Press, Oxford, (1973) 76.
[13] C. L. Fu and M. H. Yoo: Phil. Mag. Lett., 58 (1988) 199.
[14] C. L. Fu: J. Mater. Res., 5 (1990) 971.
[15] M. H. Yoo, J. A. Horton, and C. T. Liu: Oak Ridge National Laboratory Report, ORNL/TM-10709, July, 1988.
[16] H. Yasuda, T. Takasugi, and M. Koiwa: Mater. Trans. JIM, 32 (1991).
[17] B. Verlinden, T. Suzuki, L. Delacy, and G. Guenin: Scripta Met. 18 (1984) 975.
[18] N. Rusovic and H. Warlimont: Phys. Stat. Sol. (a) 44 (1977) 609.

[19] K. Enami, J. Hasunuma, A. Nagasawa, and S. Nenno: Scripta Met., 10 (1976) 879.
[20] H. N. Leamy, E. D. Gibson, and F. X. Kayser: Acta. Met., 15 (1967) 1827.
[21] G. M. McManus: Phys. Rev., 129 (1963) 2004.
[22] Z. Nishiyama: Martensitic Transformation, Eds. by Z. Nishiyama, M. Meshii, and C. M. Wayman, Academic Press, New York, (1978) 75.
[23] N. Nakanishi: Prog. Mater. Sci., 24 (1980) 143.
[24] S. G. Lekhnitskii: Theory of Elasticity of an Anisotropic Elastic Body, Holden Day, San Francisco, (1963).
[25] C. L. Fu and M. H. Yoo: Phil. Mag. Lett., 62 (1990) 159.
[26] M. H. Yoo, C. L. Fu, and J. K. Lee: High-Temperature Ordered Intermetallic Alloys IV, MRS Symp. Proc., Eds. by J. O. Stiegler, L. Johnson, and D. P. Pope, (1991) (in press).
[27] M. H. Yoo and B. T. M. Loh: J. Appl. Phys., 41 (1970) 2805.
[28] Y. Minonishi and M. H. Yoo: Phil. Mag. Lett., 61 (1990) 203.
[29] L. E. Malvern: Introduction to the Mechanics of a Continuous Medium, Prentice Hall, Englewood Cliffs, N.J., (1969) 217.
[30] J. P. Hirth and J. Lothe: Theory of Dislocations, McGraw-Hill, New York, (1982) 91.
[31] M. H. Yoo: High-Temperature Ordered Intermetallic Alloys II, Eds. by N. S. Stoloff, C. C. Koch, C. T. Liu, and O. Izumi, MRS Symp. Proc., Vol 81 (1987) 207.
[32] M. H. Yoo and B. T. Loh: J. Appl. Phys., 42 (1972) 1373.
[33] T. Yamagata and H. Yoshida: Mater. Sci. Eng., 12 (1973) 95.
[34] J. D. Eshelby: Phil. Mag., 40 (1949) 903.
[35] T. Suzuki, Y. Mishima, and S. Miura: ISIJ International, 29 (1989) 1.
[36] P. H. Thornton, R. G. Davies, and T. L. Johnson: Met. Trans., 1 (1970) 207.
[37] R. A. Mulford and D. P. Pope: Acta. Met., 21 (1973) 1375.
[38] B. H. Kear and J. M. Oblak: J. Physique, C7 (1974) 35.
[39] M. H. Yoo, Acta. Met., 35 (1987) 1559.
[40] S. Takeuchi and E. Kuramoto: Acta. Met., 21 (1973) 415.
[41] B. H. Kear and H. G. F. Wilsdorf: Trans. TMS-AIME, 224 (1962) 382.
[42] M. H. Yoo: Scripta. Met., 20 (1986) 915.
[43] J. H. Schneibel and E. P. George: Scripta Met., 24 (1990) 1069.
[44] G. C. Sih, P. C. Paris, and G. R. Irwin: Int. J. Fracture Mech., 1 (1965) 189.
[45] M. H. Yoo: J. Mater. Res., 4 (1989) 50.
[46] M. H. Yoo, C. L. Fu, and J. K. Lee: J. Phys. III, 1 (1991), to appear in March Special Issue Mechanisms of Deformation and Strength in Advanced Materials, Aussois, France (1990).
[47] M. Yamaguchi, V. Vitek, and D. P. Pope: Phil. Mag. A, 43 (1981) 1027.
[48] M. Yamaguchi, D. P. Pope, and V. Vitek: Phil. Mag. A, 43 (1981) 1265.
[49] P. M. Anderson and J. R. Rice: Scripta Met., 20 (1986) 1467.
[50] Z. C. Yao, Ph.D. Thesis, Ohio State University (1990).